arXiv:1512.03137v1 [gr-qc] 10 Dec 2015

Toward terrestrial detection of millihertz gravitational waves with magnetically assisted torsion pendulums

Eric Thrane,[a] R. P. Anderson, Yuri Levin, and L. D. Turner
School of Physics and Astronomy, Monash University, Clayton, Victoria 3800, Australia
(Dated: December 11, 2015)

Current terrestrial gravitational-wave detectors operate at frequencies above 10 Hz. There is strong astrophysical motivation to construct low-frequency gravitational-wave detectors capable of observing 10–10^4 mHz signals. However, there are numerous technological challenges. In particular, it is difficult to isolate test masses so that they are both seismically isolated and freely falling under the influence of gravity at mHz frequencies. We propose a Magnetically Assisted Gravitational-wave Pendulum Intorsion (MAGPI) suspension design for use in low-frequency gravitational-wave detectors. We construct a noise budget to determine the required specifications. In doing so, we identify what are likely to be a number of limiting noise sources for terrestrial mHz gravitational-wave suspension systems. We conclude that it may be possible to achieve the required seismic isolation and coupling to gravitational waves necessary for mHz detection, though, there are significant experimental challenges.

Introduction. Second-generation gravitational-wave detectors [1–3] observe at frequencies above $f \approx 10\,\mathrm{Hz}$. This is because the test masses are suspended with linear pendulums with resonant frequencies $\approx 1\,\mathrm{Hz}$, which isolate the test masses from seismic noise. They also ensure that the test masses behave as though they are freely falling, which allows them to move under the influence of gravitational waves. However, both seismic suppression and coupling to gravitational waves are only effective above the resonant frequency. Below the resonant frequency, seismic noise is not attenuated and the coupling to gravitational waves falls rapidly.

However, there is strong astrophysical motivation to design gravitational-wave detectors that can operate at lower frequencies [4]:

1. Gain sensitivity to intermediate-mass black-hole mergers with total mass $\gtrsim 1600 M_\odot$.
2. Improve sensitivity to stochastic backgrounds. Since the stochastic search signal-to-noise ratio scales like f^{-3}, it is possible to achieve a dramatic improvement in sensitivity by expanding the observation band to include lower frequencies [5].
3. Gain sensitivity to the ≈80% of pulsars that emit gravitational waves with $f < 10\,\mathrm{Hz}$—out of the reach of audio-band detectors [6].
4. Improve low-latency follow-up alerts by gaining an advanced inspiral signal prior to merger [7].

Despite this strong motivation, it is not easy to modify current detectors that are based on linear pendulums to probe frequencies below 10 Hz. This is because the resonant period of a linear pendulum scales with the square root of its length, and extremely long pendulums (length $\gg 1\,\mathrm{m}$) are impractical.

The attenuation of seismic noise, and the coupling of gravitational waves to a suspended test mass, can each be described by transfer functions. For a linear pendulum, the seismic transfer function relating displacement noise x_t (at the top suspension point from which the pendulum is hung) to displacement of the test mass at the bottom x_b is given by

$$T_s(f) = \frac{x_b}{x_t} = \frac{f_0^2}{f_0^2 - f^2}, \tag{1}$$

where f is the measured gravitational-wave frequency and f_0 is the resonant frequency of the linear pendulum.

The acceleration from a gravitational wave on an interferometer test mass can be written as $a_h = -4\pi^2 f^2 h L$ where h is the gravitational-wave strain and L is the length of the interferometer arms. For a linear pendulum, the gravitational-wave transfer function relating h to the measured strain x_b/L is given by:

$$T_h(f) = \frac{x_b}{hL} = \frac{f^2}{f^2 - f_0^2}. \tag{2}$$

In Fig. 1 we plot $T_s(f)$ (solid) and $T_h(f)$ (dashed) for a (typical) 1 m linear pendulum with $f_0 = 0.5\,\mathrm{Hz}$ in blue. We see that below f_0, the test mass is not isolated from seismic noise, and the coupling to gravitational waves falls like f^2.

A magnetically assisted torsion pendulum. In this Letter we propose a magnetically assisted torsion pendulum for use in a LIGO-like interferometer. We refer to this scheme as Magnetically Assisted Gravitational-wave Pendulum Intorsion (MAGPI). Torsion pendulums are widely used in precision measurement because they can be made with very low resonant frequencies $f_0 \lesssim 1\,\mathrm{mHz}$ and with very high quality factors $Q \approx 10^4$ [8, 9]. Ando *et al.* have previously noted that a pair of torsion pendulums can be coupled to tidal deformations from gravitational waves, thereby exploiting the naturally low resonance frequency of torsion pendulums [10]. However, the sensitivity of the detector is limited by the 10 m length of

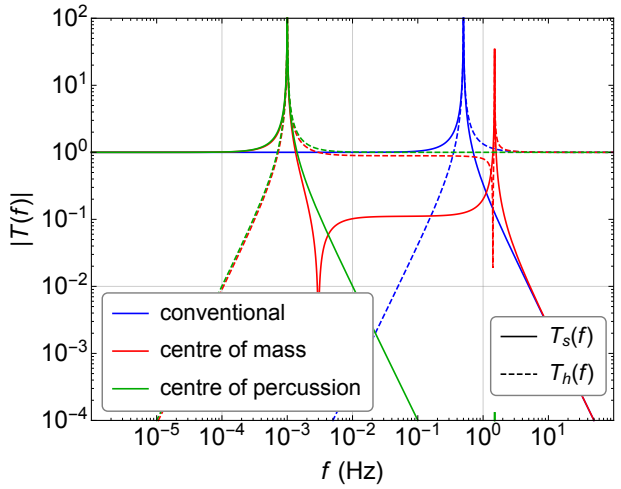

FIG. 1. Transfer functions for seismic noise (solid) and gravitational waves (dashed). Blue is for a linear pendulum with resonant frequency $f_0 = 0.5\,\mathrm{Hz}$, red is for the center of mass in a magnetically assisted (MAGPI) pendulum $f_r = 1\,\mathrm{mHz}$, and green is for the MAGPI center of percussion, offset from the center of mass.

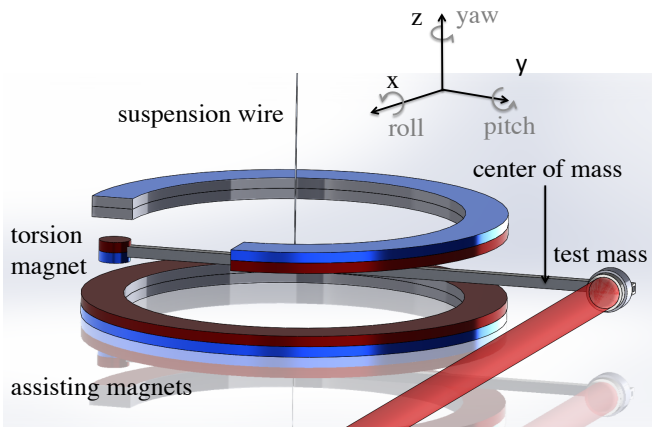

FIG. 2. Schematic of the Magnetically Assisted Gravitational-wave Pendulum Intorsion (MAGPI); not to scale, with a sector of the upper assisting magnet made invisible. The assisting magnets exert a force on the torsion bar magnet, which holds up the bar. Without this torque, the bar would hang vertically. Gravitational-wave strain, acting on the center of mass, induces motion in the yaw degree of freedom.

the torsion bars. See also [11] for a discussion of maglev-based suspension.

A schematic of the MAGPI design is provided in Fig. 2. We employ an asymmetric, unbalanced torsion bar with a test mass on one side and a much less massive permanent magnet on the other side. We refer to this magnet as the "torsion magnet" to distinguish it from the "assisting magnets," that exert a vertical magnetic force $\vec{F} = \mu\vec{\nabla}B_z$ on the torsion bar to hold it horizontal. Here, $\vec{\mu} = \mu\hat{z}$ is the magnetic moment of the torsion magnet and $\vec{B}$ is the magnetic field of the assisting magnets. Identical MAGPIs are situated at the ends of each arm of a Michelson interferometer. The torsion bar and the assisting magnets are both suspended from a pre-isolation system consisting of a suspension-point interferometer and an optically rigid body as in [4]. In Fig. 2, a mirror mounted on the test mass reflects light in the $\hat{x}$ direction, down the interferometer arm.

In this asymmetric configuration, the center of mass is offset from the lower suspension point in the $\hat{y}$ direction, and so a gravitational wave will couple to the torsional (yaw) degree of freedom by exerting a torque on the bar. As a consequence, the test mass behaves as though it is suspended by a low-resonant-frequency torsion pendulum, greatly expanding the frequency range over which gravitational waves can be measured. To illustrate this, we calculate the seismic transfer function $T_s'(f)$ and the gravitational-wave transfer function $T_h'(f)$ for the MAGPI design. The prime distinguishes the MAGPI transfer functions from those of the conventional linear pendulums discussed above.

For illustrative purposes, we assume the following fiducial parameters. The test mass is $m = 100\,\mathrm{kg}$. The mass of the bar and the torsion magnet are assumed to be small in comparison. The distance between the lower suspension point and the center of mass is $r = 50\,\mathrm{cm}$. For reasons described below, the test mass is placed 56 cm away from the lower suspension point, 6 cm beyond the center of mass. In order to minimize noise from eddy currents, the magnets are constructed from a high-remanence, ferrimagnetic insulator such as yttrium iron garnet (YIG).

Considering the total force on the center of mass yields the following equation of motion:

$$-f^2 x_m = -f_0^2(x_m + r\phi - x_t) - f^2 L h, \qquad (3)$$

where x_m is the displacement of the center of mass along $\hat{x}$, f is frequency, $f_0 = 0.5\,\mathrm{Hz}$ is the resonant frequency of the linear pendulum degree of freedom, x_t is the seismically-induced displacement at the upper suspension point along $\hat{x}$, and ϕ is the (right-hand) yaw angle about the $\hat{z}$ axis. Considering the total torque about the center of mass yields another equation of motion:

$$-If^2\phi = -rmf_0^2(x_m + r\phi - x_t) - I_z f_r^2 \phi. \qquad (4)$$

Here, $f_r \approx 1\,\mathrm{mHz}$ is the rotational resonant frequency of the torsion pendulum, I is the yaw moment of inertia about the center of mass, and $I_z \approx I + mr^2$ is the moment of inertia about the lower suspension point.

Combining Eqs. 3-4, we obtain the transfer functions:

$$\begin{aligned} T_s'(f) \equiv \frac{x_m}{x_t} &= \frac{f_0^2\left(\kappa f_r^2 - f^2\right)}{f^4 - f^2\kappa\left(f_0^2 + f_r^2\right) + \kappa f_0^2 f_r^2} \\ T_h'(f) \equiv \frac{x_m}{hL} &= \frac{f^2\left(f^2 - \kappa\left(f_0^2 + f_r^2\right) + f_0^2\right)}{f^4 - \kappa f^2\left(f_0^2 + f_r^2\right) + \kappa f_0^2 f_r^2} \end{aligned} \qquad (5)$$

Here, we introduce $\kappa = mr^2/I + 1$, which becomes larger as mass is more efficiently concentrated around the center of mass. For our design, $\kappa \approx 9$.

In Fig. 1, we plot $T_s'(f)$ (solid) and $T_h'(f)$ (dashed) in red. We see that the test mass behaves as though it is freely falling (along $\hat{x}$) above $f_r = 1\,\mathrm{mHz}$. However, the seismic noise between (f_r, f_0) is only suppressed by a factor of ≈ 9. In order to further attenuate seismic noise, we consider a point some distance δr beyond the center of mass known as the center of percussion:

$$\delta r = \frac{r}{\kappa - 1}\left(1 - \kappa\frac{f_r^2}{f_*^2}\right). \tag{6}$$

At the center of percussion, the seismic coupling is zero when $f = f_*$. Physically, the test mass is at rest while the bar rotates back and forth about it. We treat f_* as a tunable parameter that varies with δr. However, the best broadband suppression of seismic noise occurs when $f_* \gg f_r$, in which case $\delta r \to r/(\kappa - 1)$. For the design considered here, $\delta r = 6\,\mathrm{cm}$.

At the center of percussion, the transfer functions become

$$\begin{aligned} T_s''(f) &= \frac{\kappa f_0^2 f_r^2\left(f_*^2 - f^2\right)}{f_*^2\left(f^4 - \kappa f^2\left(f_0^2 + f_r^2\right) + \kappa f_0^2 f_r^2\right)} \to -\frac{f_r^2}{f^2} \\ T_h''(f) &= \frac{f^2(f_*^2(f^2 - \kappa(f_0^2 + f_r^2)) + \kappa f_0^2 f_r^2)}{f_*^2\left(f^4 - \kappa f^2\left(f_0^2 + f_r^2\right) + \kappa f_0^2 f_r^2\right)} \to 1 \end{aligned} \tag{7}$$

The double-prime denotes that we are considering motion at the center of percussion and not the center of mass. The arrows in Eq. 7 show the behavior in the limit that $f_0, f_* \gg f > f_r$. Thus, a test mass placed at the center of percussion behaves as though it is suspended from a linear pendulum with resonant frequency f_r. In Fig. 1, we plot $T_s''(f)$ (solid) and $T_h''(f)$ (dashed) for the MAGPI center of percussion (green). It is interesting to consider this behavior qualitatively. At frequencies below the linear pendulum resonance, the lower suspension point behaves as though it is rigidly attached. Forces acting on the center of mass cause the test mass to yaw around the lower suspension point.

There are several possibly-limiting noise sources for low-frequency gravitational-wave detectors including thermal noise, Newtonian gravity gradient noise, and radiation pressure noise [4]. For the sake of comparison, we assume that our MAGPIs are installed in an $L = 300\,\mathrm{m}$ Michelson interferometer as per the MANGO design described in [4]. We further assume that the MAGPIs operate with a resonant frequency of $f_r = 1\,\mathrm{mHz}$ so that seismic noise can be suppressed by the previous stages in the MANGO design: a suspension-point interferometer from which is hung an optically rigid body [4]. (The assisting magnets are suspended in addition to the torsion bar.) The optically rigid body eliminates most seismic noise through a servo, which also eliminates gravitational-wave induced motion in the isolation stage. The final MAGPI stage is necessary so that the test mass couples to gravitational waves. We ignore Newtonian gravity gradient noise likely common to any terrestrial detector; see [12] for a possible mitigation strategy.

Our noise budget is shown in Fig. 3. In the MANGO design, the limiting noise below 30 mHz is due to suspension thermal noise (blue); above 30 mHz the limiting noise is quantum noise (purple). The total noise is given by the black curve. We use the MANGO estimates for these two noise sources as our starting point and investigate if the MAGPI design induces additional noise above this noise floor.

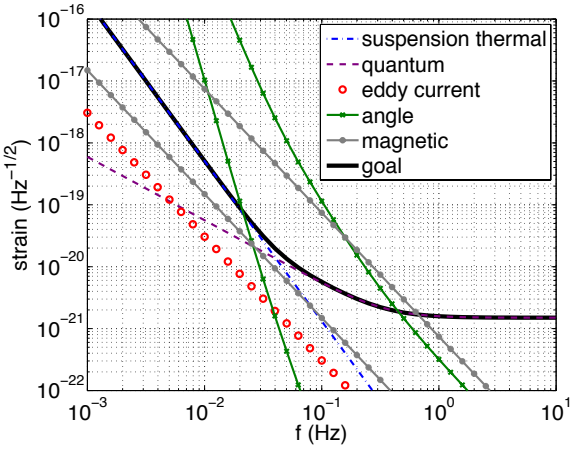

FIG. 3. MAGPI noise budget. The dashed purple dash-dot blue curves are the assumed quantum noise and the suspension thermal noise taken from [4]. The quadrature sum of these noises is the thick black line labeled "goal": we seek to avoid introducing noise above this level. The red ∘ show the expected noise from eddy currents. The green × show a range of possible noise from angular misalignment. The upper curve shows the noise if the MAGPI tilts along with the pre-isolation stage whereas the lower curve assumes that the MAGPI is further isolated by a mechanical filter with a resonant frequency of 1 mHz; see the text for details. The gray • show a range of possible noise from ambient magnetic fields. The upper curve assumes a magnetic gradient noise of $0.1\,\mathrm{fT/m/Hz^{1/2}}$ achieved with a magnetic shield. The lower curve assumes that the magnetic noise is further reduced by a factor of 50, e.g., with feed-forward; see the text for details.

Dissipation by eddy currents is a significant concern for any low-noise system utilizing strong magnetic fields. Using the fluctuation-dissipation theorem, we investigate the scaling laws for eddy current noise following the formalism from [13]. The strain noise from eddy currents dissipated in the bar magnet can be expressed as

$$\sigma_h \approx c\frac{1}{L}\sqrt{8k_B T\sigma(\pi R^2 z)}\left(\frac{B}{m\,\omega^2}\right). \tag{8}$$

Here, k_B is the Boltzmann constant, $T = 293\,\mathrm{K}$ is temperature, $R \approx 2\,\mathrm{cm}$ is the radius of the torsion magnet, $z \approx 2\,\mathrm{cm}$ is the height of the torsion magnet, σ is the

conductivity of the magnets, and $c \lesssim 1$ is a geometric constant. We assume that the distance from the suspension point to the bar magnet is $\approx r + \delta r$. In order to obtain a very rough estimate, we set $c = 1$.

Ferrimagnetic material such as YIG has both a large remanence and a low conductivity: $\sigma \approx 10^{-11}\,\mathrm{S/m}$ at $T = 293\,\mathrm{K}$, meaning that it can support a relatively large magnetic field while suppressing eddy currents [14]. Given these assumptions, the eddy current noise in the bar magnet is $\sigma_h \lesssim 10^{-22}\,\mathrm{Hz}^{-1/2}$ at $f = 0.1\,\mathrm{Hz}$: well below other sources of noise.

Eddy current noise also arises from dissipation in the assisting magnets. The volume of the assisting magnets is bigger than the volume of the torsion magnet, but the magnetic field is only large near the torsion magnet. As a very rough approximation, therefore, we assume that the eddy current noise from each assisting magnet is about the same as from the torsion magnet; (the total eddy current noise is three times the expression in Eq. 8). Our rough approximation of the total eddy current noise is indicated with red circles in Fig. 3. We note that eddy current noise can be further reduced ($\gtrsim 10\times$) through the use of laminations of the kind used in electrical transformers.

While eddy current dissipation in the ferrite magnets may not be a significant noise source, Eq. 8 tells us that there are strict constraints on the proximity of conductors. The conductivity of typical conductors such as copper is $6 \times 10^7\,\mathrm{S/m}$, eighteen orders of magnitude greater than YIG. It is therefore difficult to envision an experimental apparatus in which conductors are used for actuation, e.g., electrostatic drives. We therefore hypothesize that it is necessary to carry out all actuation with other technology, e.g., radiation pressure [15].

Angular alignment noise, e.g., from tilt, has been previously identified as a limiting noise source for purely mechanical low-frequency suspension systems [16]. For the MAGPI design, a non-zero pitch angle θ in any magnet (either the assisting magnets or the torsion magnet) will couple into the gravitational-wave channel via a yaw torque. Alignment noise $\sigma_\theta(f)$ describes fluctuations in the pitch angle of the magnets. The transfer function $T_\theta(f) = h/\theta$ is

$$T_\theta(f) \approx \left(\frac{r + \delta r}{L}\right)\left(\frac{f_\theta^2}{f_r^2 - f^2}\right) \tag{9}$$

where $f_\theta = \sqrt{g/r}/2\pi \approx 500\,\mathrm{mHz}$ and g is the acceleration due to gravity. The factor of g appears because the magnetic torque is tuned to balance the gravitational torque. The fact that $f_\theta \gg f_r$ implies that alignment noise will tend to be amplified through most of the observing band. This places strict requirements on tilt noise.

The pre-isolation stage limits $\sigma_\theta(f)$ using active feedback. By measuring the $\hat{x}$ displacement of the bottom and top of the optically rigid body, θ can (at best) be measured with uncertainty $\sigma_\theta = \sqrt{2}(\sigma_h L/\ell)$, where σ_h is the total strain MANGO sensitivity and $\ell \approx 1\,\mathrm{m}$ is the vertical distance between the bottom and top measuring points. When $f = f_\theta$, $\sigma_\theta \approx 8 \times 10^{-19}\,\mathrm{rad/Hz^{1/2}}$.

The transfer function describing how tilt at the pre-isolation stage θ_1 couples to the tilt of the MAGPI magnets θ_2 is $T'_\theta(f) = (f'_\theta/f)^2$. Here, $f'_\theta = \sqrt{\mathfrak{r} mg/I_y}/2\pi$ depends on the distance between the center of mass and the suspension point $\mathfrak{r}$ and the pitch moment of inertia about the lower suspension point I_y. Angular alignment noise can be reduced by making $\mathfrak{r}$ small, which reduces f'_θ. (Tilt noise is converted into displacement noise at the suspension point.) Here, we suppose that $f'_\theta = 1\,\mathrm{mHz}$, an optimistic but plausible value. The green traces in Fig. 3 show σ_h^θ at the pre-isolation stage (top) and after coupling to the MAGPI magnets (bottom).

We anticipate alignment noise is a general problem for assisted pendulums because fluctuations in the assisting force will always couple at some level to the strain degree of freedom. We hypothesize that, for any design, there is no "free lunch": the natural frequency of the assisting force will be close to the natural frequency of the unassisted pendulum, and that noise coupling through this mechanism will grow at low-f like $\sigma_h \propto 1/f^2$.

Ambient magnetic fields from geophysical and anthropogenic sources create fluctuations at the level of $\sigma_B \approx 1\,\mathrm{pT/Hz^{1/2}}$ in our frequency band [17]. Shielding can reduce magnetic noise to $\sigma_B \lesssim 1\,\mathrm{fT/Hz^{1/2}}$ [18]. Thanks to the orientation of the torsion magnet, *uniform* magnetic fields do not efficiently couple to the yaw degree of freedom because the torque $\vec{\mu} \times \vec{B}$ is perpendicular to the $\hat{z}$ axis. However, magnetic field *gradient* noise couple via:

$$-m\omega^2 hL = \mu \nabla_x B_z. \tag{10}$$

In order to ensure that ambient magnetic fields are not a limiting noise source, it is necessary to limit the magnetic gradient to be $\nabla_x B_z \lesssim 2 \times 10^{-3}\,\mathrm{fT/Hz^{1/2}}$. (Here, we have assumed a magnetic moment of $\mu = 9\,\mathrm{J/T}$.) Thus, a magnetic shield, placed at a distance of $\approx 10\,\mathrm{m}$ from the torsion magnet, may produce gradients $\lesssim 50\times$ above the required noise level.

We consider two strategies to further reduce magnetic noise. The first is to precisely measure the ambient magnetic field in order to subtract out the resulting strain noise. Warm atomic vapor magnetometers are currently capable of measuring magnetic fields with sensitivities of $0.5\,\mathrm{fT/Hz^{1/2}}$ [19]. By scaling these sensors to larger volumes, it may be possible to accurately measure residual magnetic gradient noise inside the shielded cavity so that the resulting yaw noise can be canceled by a servo.

The second strategy is to replace each magnetic component with multiple magnets of alternating polarity such that the net magnetic moment of both is zero. In principle, this can be achieved while still obtaining the magnetic force used to levitate the torsion bar. With

this design, the MAGPI would be sensitive to the second spatial derivative of the magnetic field, potentially reducing the magnetic noise by a factor of $\gtrsim 10$ depending on the thickness of the alternating magnets and the precision with which they can be constructed. The gray • in Fig. 3 show different magnetic noise scenarios. The upper trace shows the magnetic noise limited only by a magnetic shield. The lower trace shows the target magnetic noise, reduced through some other means by a factor of 50.

Additional noise sources are possible as well. We discuss a few while acknowledging that our list is certainly incomplete. First, the motion of the torsion magnet in the external field may incur dissipation through hysteresis. Second, additional work is required to estimate noise from the Barkhausen effect. Third, there is dissipation associated with mechanical stress and strain, especially from resonances created from the attachment of the mirror/magnets to the torsion bar. Fourth, a follow-up study is necessary to understand magneto-mechanical interactions between the torsion bar and the assisting magnets. Fifth, DeSalvo argues that dislocation dislocation self organized criticality (SOC) noise is a limiting noise source for torsion pendulums [20]. However, it might be mitigated through the use of glassy metals. Further work is required to determine the relative importance of these noise sources. Barkhausen noise is of particular concern given experience from Initial LIGO [21].

Conclusions. We have outlined a pathway by which it may be possible to construct suspension systems for mHz gravitational waves with terrestrial detectors. However, significant experimental challenges must be overcome to realize a working MAGPI. While our proposal (and TOBA [10]) utilize the natural resonant frequency of a torsion pendulum, other designs seek to achieve low resonant frequency suspensions using magnetic levitation controlled via active feedback [22, 23]. Because of the large magnetic fields required for magnetic levitation, eddy current dissipation is an important design challenge. Future work will focus on development of a small-scale prototype to test the fundamental principles of the MAGPI design including the seismic isolation and the coupling to a driving force (a simulated gravitational wave) acting on the center of mass. We also leave for future work the calculation of other more subtle noise sources such as dissipation through hysteresis in the torsion magnet.

We thank Riccardo DeSalvo and Vuk Mandic for discussions, which got us thinking about the problem of low-frequency suspension; Todd Wagner, Vladimir Dergachev, Bram Slagmolen, Rana Adhikari, and John Winterflood for advice; and Lawrie Hanson for the MAGPI acronym.

[a] eric.thrane@monash.edu

[1] J. Abadie *et al.*, Classical Quantum Gravity **32**, 074001 (2015).
[2] F. Acernese *et al.*, Classical Quantum Gravity **32**, 024001 (2015).
[3] Y. Aso, Y. Michimura, K. Somiya, M. Ando, O. Miyakawa, T. Sekiguchi, D. Tatsumi, and H. Yamamoto, Phys. Rev. D **88**, 043007 (2013).
[4] J. Harms, B. J. J. Slagmolen, R. X. Adhikari, M. C. Miller, M. Evans, Y. Chen, H. Müller, and M. Ando, Phys. Rev. D **88**, 122003 (2013).
[5] B. Allen and J. D. Romano, Phys. Rev. D **59**, 102001 (1999).
[6] G. Hobbs, R. N. Manchester, and L. Toomey, "ATNF Pulsar Catalogue, v1.53," (2015).
[7] K. Cannon, R. Cariou, A. Chapman, M. Crispin-Ortuzar, N. Fotopouls, M. Frei, C. Hanna, D. Keppel, and L. Liao, Astrophys. J. **748**, 136 (2012).
[8] C. A. Hagedorn, S. Schlamminger, and J. H. Gundlach, in *6th International LISA Symposium*, AIP Conference Proceedings, Vol. 873, edited by S. Merkowitz and J. Livas (American Institute of Physics, Melville, NY, 2001).
[9] E. Adelberger, J. H. Gundlach, B. R. Heckel, S. Hoedl, and S. Schlamminger, Prog. in Part. and Nucl. Phys. **62**, 102 (2009).
[10] M. Ando, K. Ishidoshiro, K. Yamamoto, K. Yagi, W. Kokuyama, K. Tsubono, and A. Takamori, Phys. Rev. Lett. **105**, 161101 (2010).
[11] G. Mamakoukas, H. Miao, K. Arai, and R. Adhikari, "Sensing and control of a six-DOF maglev-based suspension prototype," (2013).
[12] J. C. Driggers, J. Harms, and R. X. Adhikari, Phys. Rev. D **86**, 102001 (2012).
[13] Y. Levin, Phys. Rev. D **57**, 659 (1998).
[14] L. Sirdeshmukh, K. K. Kumar, S. B. Laxman, A. R. Krishna, and G. Sathaiah, Bull. Mater. Sci. **21**, 219 (1998).
[15] E. Goetz, P. Kalmus, S. Erickson, R. L. Savage, G. Gonzalez, K. Kawabe, and M. Landry, Classical Quantum Gravity **26**, 245011 (2009).
[16] F. Garoi, J. Winterflood, L. Ju, J. Jacob, and D. G. Blaire, Rev. Sci. Instrum. **74**, 3487 (2003).
[17] J. Marfaing *et al.*, Europhys. Lett. **88**, 19002 (2009).
[18] T. W. Kornack, S. J. Smullin, S.-K. Lee, and M. V. Romalis, Applied. Phys. Lett. **90**, 223501 (2007).
[19] D. Sheng, S. Li, N. Dural, and M. V. Romalis, Phys. Rev. Lett. **110**, 160802 (2013).
[20] R DeSalvo, Phys. Lett. A **379**, 1202 (2015).
[21] A. Effler *et al.*, Classical Quantum Gravity **32**, 035017 (2015).
[22] M. Varvellaa, E. Callonia, L. D. Fiorea, L. Milanoa, and N. Arnaudb, Astropart. Phys. **21**, 325 (2004).
[23] R. W. P. Drever, in *Dark Matter in Cosmology Quantum Measurements Experimental Gravitation*, edited by R. Ansari, Y. Giraud-Heraud, and J. T. T. Van (Editions Frontières, Gif-sur-Yvette, France, 1996) p. 375.